IIETA International Information and Engineering Technology Association
Advancing the World of Information and Engineering

Mathematical Modelling of Engineering Problems
Vol. 12, No. 12, December, 2025, pp. 4225-4234
Journal homepage: http://iieta.org/journals/mmep

# Using of Hydrological and Climatic Modeling to Estimate Future Runoff Reaching the Euphrates River from Hiqlan Valley

Wisam Abdulabbas Abidalla[1*], Basim Sh. Abed[2]

[1] Department of Water Resources Engineering, College of Engineering, University of Baghdad, Baghdad 10071, Iraq
[2] Department of Civil Engineering, Al-Hadi University, Baghdad 10011, Iraq

Corresponding Author Email: wessam.abd2310@coeng.uobaghdad.edu.iq



https://doi.org/10.18280/mmep.121211

**Received:** 5 September 2025
**Revised:** 9 December 2025
**Accepted:** 15 December 2025
**Available online:** 31 December 2025

***Keywords:***
*water resource management, Hiqlan Valley, climate change, LARS.WG model, SWAT model*

**ABSTRACT**

In this study, a hydrological model and a statistical weather generation model were used to estimate future surface runoff and generate future weather elements for the Hiqlan Valley, located in the desert of the Iraqi western region. Using the climate model (LARS.WG), the weather data for the past ten years were used to generate weather data for the following ten years. The results of this model showed that maximum precipitation occurs in January, March, and December each year. These data were used as input weather data for the hydrological model: Soil and Water Assessment Tool (SWAT). Delineation of the watershed performed in the SWAT modelling yielded 17 sub-basins and 78 hydrological response units. This model simulates data representing the expected surface runoff for the next ten years for Hiqlan Valley, which reaches directly towards the Euphrates River at an outflow location (15 km downstream) from d/s of Hadith dam as an additional amount of water in the rainy season. The simulation results from the SWAT simulation showed that maximum runoff occurs in January (2029) at 12.3 mm, November (2031) at 15.1 mm, and December (2030) at 13.2 mm in the winter season, and March (2034) at 14.7 mm, and April (2028) at 22.8 mm in the spring season. The runoff occurs at a rate of two to four times annually. Estimating the amount of future surface runoff for Hiqlan Valley is necessary for planning and managing the water resources of the Euphrates River basin, which has been suffering from a recent shortage of water supplies in recent years.

## 1. INTRODUCTION

The world, including the Middle East has been significantly impacted by climate change, with the water resources sector being particularly vulnerable, and Iraq is one of the countries in the region that has been notably affected which has caused a lack of water inflows of the Euphrates River reaching the Iraqi Syrian border, coupled with an increasing demand for water for various purposes, particularly irrigation. Thus, investigating alternative water resources, such as water flowing into rivers from valleys, to assess their quantities and potential utilization, becomes essential. The surface runoff or overland flow is a flow of water over the ground surface that occurs when excess rainwater, stormwater, and meltwater can no longer sufficiently infiltrate the soil, and when the soil is fully saturated. In addition, the surface runoff usually occurs because the impervious areas do not allow water to infiltrate into the soil. The Soil and Water Assessment Tool (SWAT) model can be considered one of the most efficient hydrological models for evaluating and estimating the surface runoff caused by rainfall. This model uses the Geographic Information Systems (GIS) tools for remote sensing, and the information that can be merged with the observed database to assess and estimate the quantity of surface runoff in the objective watersheds, which might help in the management and planning of water conservation measures [1, 2]. Usually, watersheds contain so-called hydrologic units bound within topographic features that allow the water to flow as surface runoff from the highest to the lowest earth's surface due to the rain's interaction and the land surface [3]. For sustainability, it is crucial to simulate the surface runoff and measure a hydrological parameter from all parts of the catchment area using modern models [4, 5] such as the SWAT model. Also, climate change affects rainfall and temperature, which affects the quantity of surface runoff that makes it extreme, especially in the arid and semi-arid regions [6, 7]. Mohammed and Hassan [8] examined climate change impact in southern Iraq using the LARS.WG model. The model simulation was based on two emission scenarios. The results showed that the annual minimum and maximum temperatures were increased in all locations investigated by approximately 6℃ at the end of the century. In contrast, precipitation projection results demonstrated a declining trend in the same study area examined.

Hassan et al. [9] studied the impact of climate change using the LARS.WG model in the western and middle of Iraq. Weather parameters downscaled, including daily minimum temperature, maximum temperature, and precipitation for future scenarios by the model. The results showed that the

average minimum and maximum temperatures were raised by approximately 0.94 to 4.98℃ at the end of the century in all analyzed locations.

Al-Kubaisi and Al-Kubaisi [10] examined the water balance of the Kubaisa Basin in the Western Iraqi Desert by employing the SWAT model. Water discharge simulations and the variables influencing them, which were used as a basis of the study investigation over the period of 1990–2023. The study's findings show that the distribution of water in the Kubaisa Basin, including the amounts of surface water, groundwater, and discharges, was estimated during the study period. Moreover, climatic data results revealed an increased trend for the total rainfall and temperature; however, the trend lines for wind speed decreased in the same simulated period.

Thus, the use of climate generation models is vital. The climate model (LARS.WG) is one of these models and is used in this study to generate weather elements such as rainfall and temperatures for future periods in the study area. In this research, SWAT and LARS.WG models were coupled to investigate the impact of climate change in one of the valleys located on the right side of the Euphrates River in the Iraqi desert area. This study aims to expect and estimate the amount of future surface runoff in Hiqlan valley for the next ten years under the effects of climate change, which flows directly to the Euphrates River. These additional amounts of water contribute to enhancing the river's supply to meet various requirements.

## 2. METHODOLOGY

### 2.1 Study area

The study area represents Hiqlan Valley, located in the desert of the Iraqi western region in Al-Anbar city. The area of this valley is about 336.27 km$^2$. Minimum elevation 108 m and maximum elevation 318 m. In rainy seasons, Hiqlan Valley discharges the runoff that collected in its watershed to the Euphrates River at the outflow point located in Haqlania District at a distance of 15 km downstream of Haditha Dam in coordinates 42.3680 E Longitude and 34.0880 N Latitude. The location of the valley outflow is shown in Figure 1.

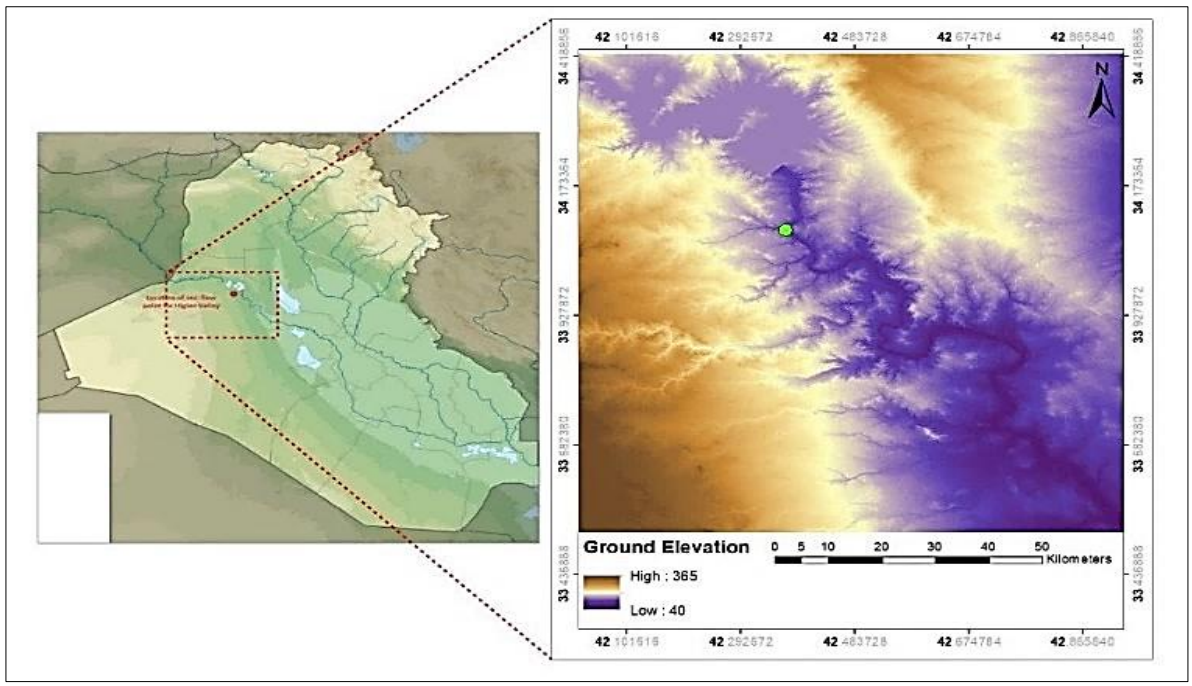


**Figure 1.** Location of outflow for Hiqlan Valley

### 2.2 Model description

2.2.1 LARS.WG model

The climate model LARS.WG is a weather generator model that is widely used in climate studies and hydrological modeling. Tools in this model are used to simulate synthetic weather data with one site under previous and future conditions and to permit the users to generate a long time series of both daily and monthly weather variables [11, 12] and make the correlation between them for approximation of the probability distributions of both wet and dry series of daily. LARS.WG model was used in this study, and the following features describe this model [13].

(1). The nature of stochastic: The LARS.WG model depends on a stochastic basis in its operation and uses randomness for the generation of weather data.

(2). The parameterization: The model requires input weather data, which is typically collected from sit weathering stations. These parameters influence the characteristics of the generated synthetic weather data.

2.2.2 SWAT model

The Rainfall-Runoff model (SWAT), which is called the "Soil and Water Assessment Tool," represents the hydrological model as a catchment, basin, or scale model and a physical model developed by "the Agricultural Research Servicers" (USDA-ARS) [12]. The SWAT-simulating process could be divided into two main parts (land and water surface). Several data inputs in model operation are required, such as digital elevation model, weather data, soil classification, vegetation, the land cover changes that occur in the watersheds, and the land use map [14, 15].

The purpose of using the SWAT model is to predict the effect of land practices management on the surface water,

sediment, and the yields of agricultural chemicals for long-term periods within a wide ungauged watershed [16]. The sub-watersheds are divided in the process of watershed delineation into several hydrological response units (HRU) to improve the simulation accuracy [17]. The SWAT model is one of the most suitable models for basin studies and is widely used in dealing with many hydrological and environmental problems. This model is used to simulate and predict the surface runoff as volume or depth. The model can be described by the following features:

(1). Inputting weather data: These data, including rain, temperature, and radiation, are required for operating the model [18]. These input data can be from previous or future periods. For the integration of using both LARS.WG with SWAT models, the results of weather data may be used as inputs for hydrological simulations. These models could simulate the impacts of the synthetic climate scenarios on the water resources and runoff, which are divided into HRUs.

(2). Soil properties: The SWAT model considers the soil properties such as texture, depth, and water retention characteristics to simulate the soil-water interactions.

(3). Land Use - Land Cover (LULC): The SWAT model incorporates the land cover with land use data to represent the distribution of the different land uses within the watershed [19]. In addition, simulates changes in both Land use and management practices.

(4). Simulating the surface runoff: The SWAT model can simulate and predict the surface runoff as volume and depth, the quantity of water out from the watershed basin through the outflow point to the nearest stream [20, 21].

## 3. MODEL INPUT DATA

### 3.1 Climate model input data

The weather data, such as precipitation and temperature for the last ten years, were collected from the Iraqi Meteorological Organization and Seismology, which are listed in Tables 1-3. Also, the Haditha weather station data, such as latitude (34.35º N), longitude (42.0º E), and altitude (140 m. a.m.s.l). These data are used in the climate model (LARS.WG) for the generation of future weather data.

The weather data is used by the climate model for generating the future weather data that is used by the hydrological model as input data for simulating and predicting the future surface runoff for Hiqlan Valley resulting from rainfall in Iraqi western, which directly reaches the Euphrates River.

**Table 1.** Monthly precipitation (mm) - period (2014–2023)

| Year | Jan. | Feb. | Mar. | Apr. | May | Jun. | Jul. | Aug. | Sep. | Oct. | Nov. | Dec. |
|---|---|---|---|---|---|---|---|---|---|---|---|---|
| 2014 | 57.3 | 10.1 | 2.6 | 11.6 | 1.7 | 0.0 | 0.0 | 0.0 | 0.0 | 2.3 | 8.6 | 6.4 |
| 2015 | 9.8 | 11.3 | 14.4 | 5.3 | 1.7 | 0.0 | 0.0 | 0.0 | 0.0 | 7.5 | 46.2 | 23.4 |
| 2016 | 1.7 | 36.3 | 21.3 | 9.3 | 0.0 | 0.0 | 0.0 | 0.0 | 0.0 | 0.0 | 1.2 | 36.1 |
| 2017 | 4.2 | 11.2 | 2.6 | 19.4 | 5.5 | 0.0 | 0.0 | 0.0 | 0.0 | 1.1 | 1.3 | 10.4 |
| 2018 | 2.8 | 5.9 | 1.5 | 7.5 | 9.4 | 0.0 | 0.0 | 0.0 | 0.0 | 3.3 | 12.4 | 34.2 |
| 2019 | 15.1 | 5.4 | 62.5 | 13.2 | 12.1 | 0.0 | 0.0 | 0.0 | 0.0 | 2.6 | 2.4 | 25.9 |
| 2020 | 12.4 | 8.3 | 38.4 | 1.6 | 3.9 | 0.0 | 0.0 | 0.0 | 0.0 | 0.00 | 8.1 | 1.1 |
| 2021 | 11.3 | 20.2 | 5.7 | 0.0 | 0.0 | 0.0 | 0.0 | 0.0 | 0.0 | 1.3 | 12.2 | 2.2 |
| 2022 | 12.2 | 17.1 | 6.7 | 0.0 | 3.7 | 0.0 | 0.0 | 0.0 | 0.0 | 1.8 | 16.5 | 15.4 |
| 2023 | 27.3 | 1.6 | 28.4 | 14.6 | 3.1 | 0.0 | 0.0 | 0.0 | 0.0 | 1.4 | 18.3 | 16.1 |

**Table 2.** Average maximum monthly temperature (°C) - period (2014–2023)

| Year | Jan. | Feb. | Mar. | Apr. | May | Jun. | Jul. | Aug. | Sep. | Oct. | Nov. | Dec. |
|---|---|---|---|---|---|---|---|---|---|---|---|---|
| 2014 | 16 | 20 | 27 | 32 | 38 | 42 | 44 | 45 | 40 | 32 | 23 | 19 |
| 2015 | 17 | 21 | 25 | 29 | 38 | 41 | 46 | 45 | 43 | 34 | 22 | 17 |
| 2016 | 16 | 22 | 27 | 32 | 37 | 42 | 45 | 47 | 40 | 35 | 25 | 15 |
| 2017 | 15 | 18 | 24 | 30 | 38 | 43 | 47 | 47 | 43 | 34 | 25 | 20 |
| 2018 | 18 | 21 | 29 | 30 | 36 | 42 | 44 | 44 | 42 | 33 | 22 | 18 |
| 2019 | 17 | 19 | 22 | 27 | 37 | 44 | 43 | 43 | 40 | 34 | 25 | 18 |
| 2020 | 17 | 19 | 24 | 30 | 47 | 45 | 45 | 44 | 41 | 34 | 24 | 17 |
| 2021 | 19 | 22 | 25 | 33 | 40 | 42 | 45 | 44 | 39 | 34 | 24 | 18 |
| 2022 | 18 | 20 | 22 | 32 | 35 | 43 | 45 | 44 | 40 | 36 | 24 | 19 |
| 2023 | 17 | 20 | 26 | 32 | 38 | 41 | 43 | 45 | 43 | 37 | 26 | 18 |

**Table 3.** Average minimum monthly temperature (°C) - period (2014–2023)

| Year | Jan. | Feb. | Mar. | Apr. | May | Jun. | Jul. | Aug. | Sep. | Oct. | Nov. | Dec. |
|---|---|---|---|---|---|---|---|---|---|---|---|---|
| 2014 | 5 | 4 | 11 | 15 | 21 | 24 | 26 | 26 | 22 | 16 | 8 | 7 |
| 2015 | 4 | 7 | 8 | 14 | 21 | 24 | 28 | 27 | 25 | 18 | 11 | 4 |
| 2016 | 4 | 7 | 11 | 15 | 21 | 25 | 27 | 27 | 22 | 16 | 8 | 3 |
| 2017 | 2 | 2 | 10 | 14 | 20 | 24 | 29 | 28 | 23 | 15 | 10 | 5 |
| 2018 | 4 | 7 | 13 | 14 | 20 | 24 | 26 | 26 | 23 | 17 | 11 | 7 |
| 2019 | 4 | 6 | 8 | 13 | 18 | 23 | 24 | 26 | 21 | 18 | 9 | 7 |
| 2020 | 4 | 5 | 11 | 15 | 18 | 23 | 25 | 26 | 22 | 18 | 10 | 6 |
| 2021 | 3 | 8 | 8 | 13 | 18 | 20 | 24 | 23 | 19 | 14 | 9 | 6 |
| 2022 | 4 | 5 | 7 | 14 | 18 | 22 | 24 | 24 | 20 | 17 | 11 | 8 |
| 2023 | 4 | 7 | 10 | 13 | 19 | 22 | 26 | 25 | 24 | 15 | 9 | 4 |

### 3.2 Hydrological model input data

For the SWAT model operation, many input data are required to predict the quantity of the surface runoff, such as digital elevation model (DEM), LULC, the soil map, and the weather data.

3.2.1 Digital elevation model

For the study area included the Hiqlan Valley, the topography was represented using DEM by the satellite imagery, as shown in Figure 2.

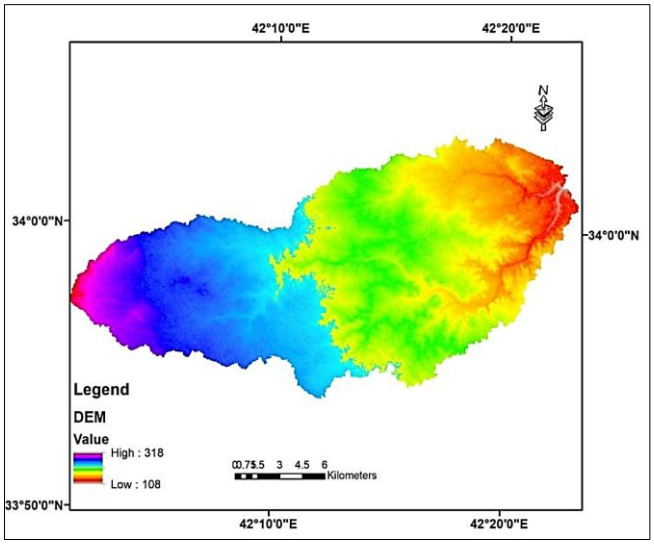


**Figure 2.** The DEM for Hiqlan Valley within the study area

3.2.2 The land use map

From the website (http://seamless.usgs), both LULC satellite images were obtained. For the process of geometrically digitizing and atmospherically correcting, the GIS was used [22, 23]. The vegetation cover in the study area has a low effect on the surface runoff because it is at a low density compared with the whole. Figure 3 illustrates the (LU-LC) land use land cover for the study area, which is classified into two main types: Agricultural Land-Row Crops, Orchid, and Corn.

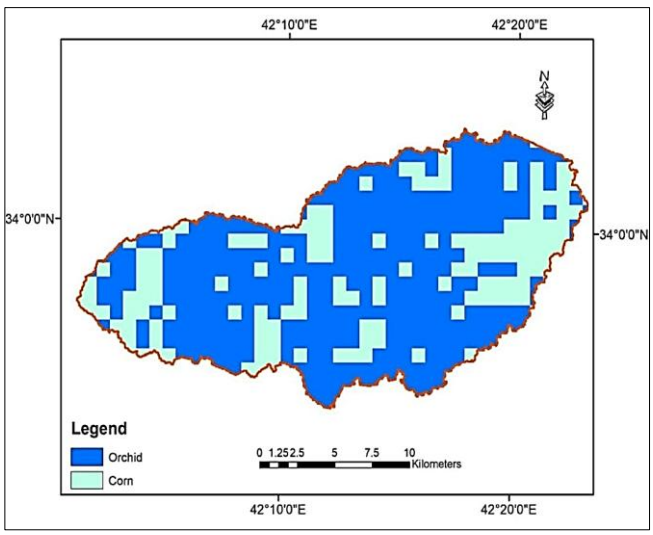


**Figure 3.** The LULC for Hiqlan Valley

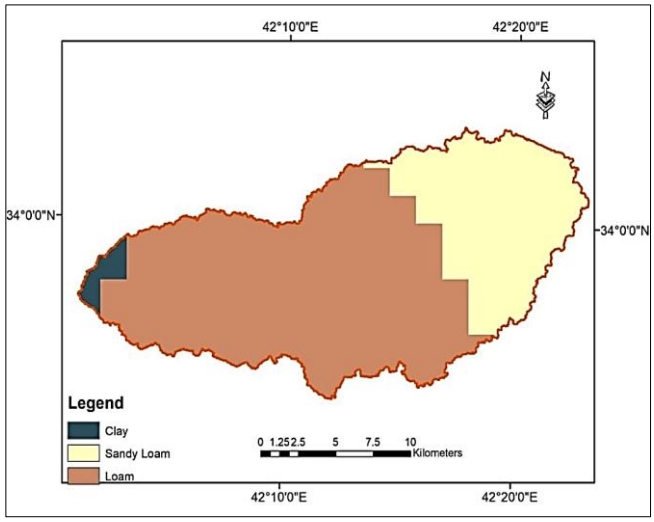


**Figure 4.** The soil map for Hiqlan Valley

3.2.3 The soil map

In watershed areas, the runoff is affected by the soil texture in terms of the porosity and permeability [24]. For agricultural purposes, the desert soils are unsuitable due to a low number of organic materials, except the alluvial soils that are nearest to the Euphrates River, which have an acceptable quantity of organic materials. By GIS, the area was registered, and the soil hydrologic group was determined using data on textural and organic matter obtained from the Food and Agriculture Organization (FAO). Figure 4 illustrates the soil map of the area of the case study.

## 4. MODEL OPERATION

The hydrological model SWAT was operated to simulate and predict the surface runoff for Hiqlan Valley, through the interface Arc SWAT. The watershed area of this valley is divided into subunits, which represent a smaller isolated unit that is characterized by the difference in physical and spatial characteristics, where the conformity of the hydrological procedures was imposed. Means that this model can divide the watershed into units that have similar characteristics in both land cover and soil, and they are placed in a similar subbasin, which is called a Hydrologic Response Unit (HRU) [25]. The map of land use and the hydrologic soil in the subunits) interior borders were used to make a unique incorporation, and it can be assumed that all incorporations, as the identical in physical properties.

### 4.1 Delineation of watershed

In watershed delineation, the DEM was used by the SWAT model. The delineation of the watershed was performed by ArcGIS with a spatial analysis [26, 27]. The description of the topography related to characterization, such as the elevation, slope, stream flow networks, creating the streamlines, the outlet points of the watershed, selecting the outlets of a watershed for both definition and calculation of sub-basin parameters, and dividing the basin into several sub-basins. In processes for delineation of watershed, the number of Sub-basins for Hiqlan Valley, equal to 17, was controlled by the number of hydrologic response units equal to 78 HRU, which depends on the value of the suitable threshold, and the nature

of the illustrated situation. For the topography of Hiqlan Valley, the maximum elevation is 318 m, the minimum elevation is 108 m, the mean is 211.4 m, and the Std. deviation is 39.493. The watershed delineation is shown in Figure 5.

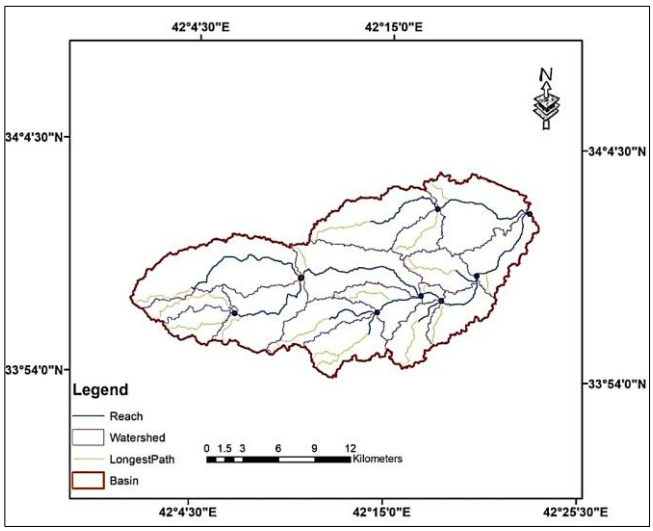


**Figure 5.** Watershed delineated for Hiqlan Valley

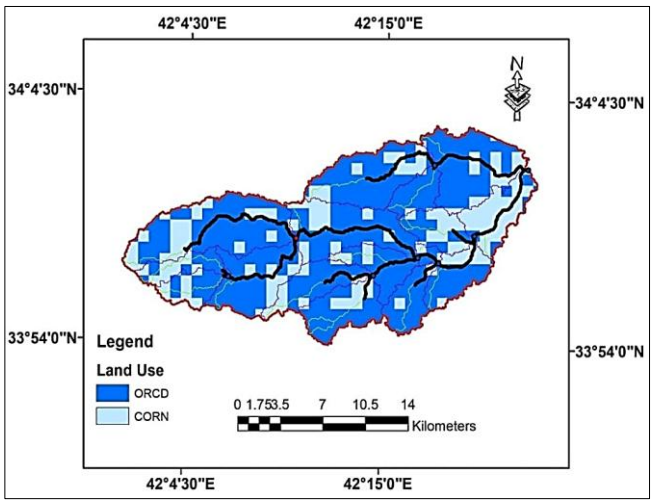


**Figure 6.** Land use reclassified by the SWAT model

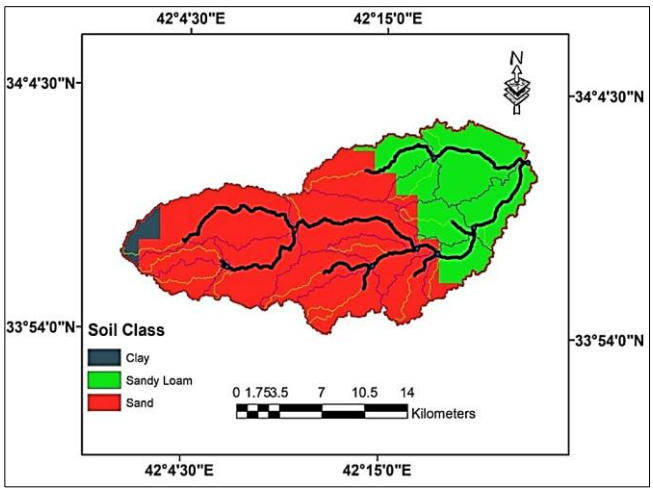


**Figure 7.** Soil reclassified by the SWAT model for Hiqlan Valley

### 4.2 Analysis of HRU

The smallest segments of a subbasin, which are specified by the changes in the soil, slope, and the classification of the LULC are called HRU [28]. The watershed was divided into areas that have a single land use with the soil incorporating that assists the model in reflecting the changing situation of hydrologic for the different land cover and soil, for raising load predictions that are accurate, with providing of best physical description in the water balancer. In the analysis of HRU, many steps were down. The first step is the insertion of the LULC map that contains classes for the land uses in the basin; these classes are matched with the Arc SWAT database classes for reclassification of the land use map. Using high-resolution images is very important in the validation of land use. In addition, matching this map and the FAO soil map with the SWAT default soil database to make the same soil classes as the soil map. This model gave the user two types of options: a single slope or multiple slopes. In this study, multiple slopes were chosen. For the last step, the overlaying was done for the soil, land use, and slope layers. At this point, the soil, land use, and slope classes were taken into account in the processing of the simulation.

#### 4.2.1 Land use reclasses

Reclassification of land use types which is one of the important performances of the SWAT model, was done to load data corresponding to the SWAT model that was informed by overlapping the satellite image of the land use with the area of the Hiqlan Valley, as shown in Figure 6.

#### 4.2.2 Soil reclasses

For the performance of the SWAT model, a reclassification of soil types was done for loading data in the corresponding SWAT model, which was informed by overlapping the satellite image of soil with the area of the Hiqlan Valley, as shown in Figure 7.

#### 4.2.3 Slope reclassified

The land slope reclassification types were done for loading data that corresponded to the SWAT model, which was informed by overlapping the satellite image of a slope with the area of the Hiqlan Valley, as shown in Figure 8.

The HRU for this valley was summarized in Table 4.

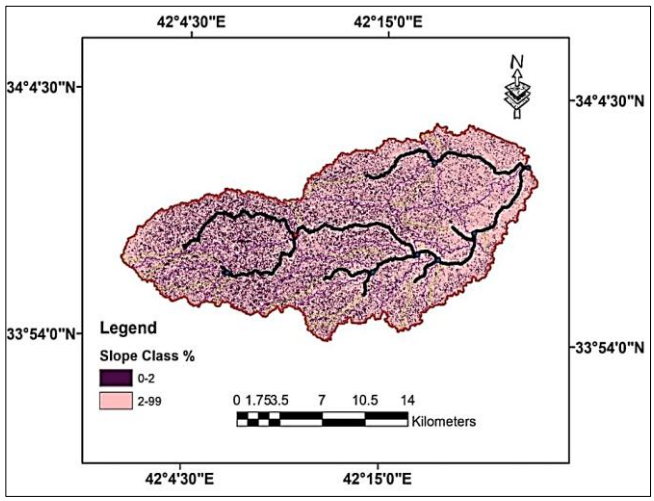


**Figure 8.** Slope reclassified by the SWAT model

**Table 4.** The analysis of HRU for the valley within the study area

| Soil Reclassification | | Land Reclassification | |
|---|---|---|---|
| **Soil Type** | **Model Area (%)** | **Land Type** | **Model Area (%)** |
| Clay | 3 | ORCD | 70 |
| Sandy Loam | 30 | CORN | 30 |
| Sand | 67 | | |

## 5. STATISTICAL TEST ANALYSIS

### 5.1 The climate model

For LARS.WG model, the autocalibration and statistical analysis are done by the model software automatically. The K-S test and p-value test show the perfect suitability of applying this model for the weather data in the study area. Statistical test analysis for precipitation and temperature is listed in Tables 5-7.

**Table 5.** K-S and p-value test for daily rain distributions

| Month | K-S | p-value | Assessment |
|---|---|---|---|
| January | 0.132 | 0.891 | V. good fit |
| February | 0.062 | 1 | Perfect |
| March | 0.051 | 0.953 | Perfect |
| April | 0.101 | 0.991 | V. good fit |
| May | 0.161 | 0.359 | Moderate fit |
| June | | N0 Rain | |
| July | | N0 Rain | |
| August | | N0 Rain | |
| September | | N0 Rain | |
| October | 0.126 | 0.992 | V. good fit |
| November | 0.168 | 0.87 | V. good fit |
| December | 0.142 | 0.965 | V. good fit |

**Table 6.** K-S and p-value test for daily (Min. Temp.) distributions

| Month | K-S | p-value | Assessment |
|---|---|---|---|
| January | 0.053 | 0.978 | Perfect |
| February | 0.095 | 0.893 | Perfect |
| March | 0.140 | 1 | V. good fit |
| April | 0.039 | 0.996 | Perfect |
| May | 0.094 | 0.932 | Perfect |
| June | 0.018 | 1 | Perfect |
| July | 0.106 | 0.999 | V. good fit |
| August | 0.158 | 0.913 | V. good fit |
| September | 0.044 | 0.966 | Perfect |
| October | 0.087 | 0.929 | Perfect |
| November | 0.017 | 1 | Perfect |
| December | 0.048 | 1 | Perfect |

**Table 7.** K-S and p-value test for daily (Max. Temp.) distributions

| Month | K-S | p-value | Assessment |
|---|---|---|---|
| January | 0.106 | 0.999 | V. good fit |
| February | 0.053 | 1 | Perfect |
| March | 0.012 | 0.965 | Perfect |
| April | 0.045 | 0.989 | Perfect |
| May | 0.093 | 1 | Perfect |
| June | 0.106 | 0.922 | V. good fit |
| July | 0.136 | 0.954 | V. good fit |
| August | 0.114 | 0.831 | V. good fit |
| September | 0.033 | 1 | Perfect |
| October | 0.106 | 0.963 | V. good fit |
| November | 0.105 | 0.948 | V. good fit |
| December | 0.044 | 1 | Perfect |

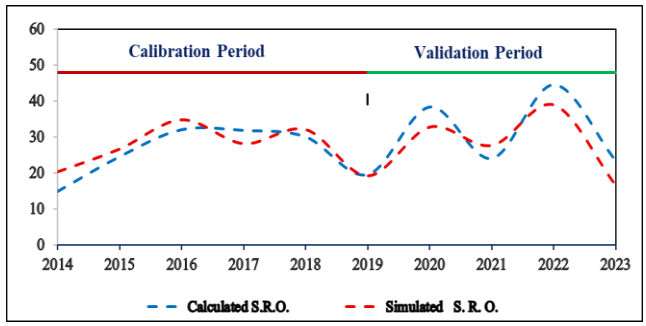


**Figure 9.** Comparison between calculated and simulated runoff for both the calibration - validation periods

### 5.2 The hydrological model

5.2.1 Suitability of applying the SWAT model

For the valleys located in the desert of Iraqi western in Anbar Governorate that reach their surface runoff in the rainy season to the Euphrates River directly in the river path extending from Hadith Dam to Ramadi city. Many researchers used the SWAT model in their studies to estimate surface runoff in those regions (valleys). Sulaiman et al. [29] demonstrated the applicability and suitability of applying the SWAT model. Because of the unavailability of observed field data about the surface runoff for Hiqlan Valley, the observed rainfall data for the period (2014–2023) were used to calculate field surface runoff data for this valley using the rainfall-runoff formula as expressed in Eq. (1).

$$Q = \frac{(P - 0.2\,S)^2}{(P + O.8\,S)} \tag{1}$$

where, $Q$ is the field surface runoff, $P$ is the rainfall, and $S$ is a parameter related to the curve number ($CN$) as expressed in Eq. (2).

$$S = \frac{1000}{CN} - 10 \tag{2}$$

A comparison was done between the calculated and simulated surface runoff, as shown in Figure 9.

5.2.2 Statistical test of the SWAT model

Statistical analysis was done to test the goodness and suitability of applying the SWAT model for Hiqlan Valley with its simulated data and calculated (from field data) for the period (2014–2023). The Calibration for six years (2014–2019) and Validation for four years (2020–2023) were conducted. Two Statistical tests (Nash-Sutcliffe (NS)) test, Eq. (3), and the coefficient of determination ($R^2$) test, Eq. (4) [30, 31], were applied for the two sets of data on Surface Runoff in both periods.

$$NS = 1 - \left[\frac{\sum_{i=1}^{n}(Y_i^{obs} - Y_i^{sim})^2}{\sum_{i=1}^{n}(Y_i^{obs} - Y_i^{mean})^2}\right] \tag{3}$$

where, $NS$ is the Nash-Sutcliffe coefficient, $Y$ is and variable, $obs$ is observed data, and $sim$ is simulated data by the model.

$$R^2 = \frac{[\sum_i (Q_{m,i} - Q_m^-)(Q_{s,i} - Q_s^-)]^2}{\sum_i (Q_{m,i} - Q_m^-)^2 \sum_i (Q_{s,i} - Q_s^-)^2} \tag{4}$$

where, $R^2$ is the coefficient of determination, $Q$ is any variable, $m$ is measured data, and $s$ is simulated data by the model. The results of these tests are listed in Table 8.

**Table 8.** Statistical testing for Hiqlan Valley of the model calibration–validation

| Evaluation of Model | NS | $R^2$ |
|---|---|---|
| Calibration - (2014–2019) | 0.70 | 0.76 |
| Validation - (2020–2023) | 0.61 | 0.68 |

From these results, the values of the NS test for both simulated and calculated data in the calibration and validation periods are somewhat similar. Also, the same goodness of results in the $R^2$ test.

## 6. RESULTS AND ANALYSIS

### 6.1 LARS-WG model results

The climate model LARS-WG used the historical weather data for the past ten years (2014–2023) to generate weather data for the next ten years (2026–2035), as shown in Figure 10 to generate the precipitation and Figures 11 and 12 to generate the maximum and minimum temperature, respectively.

Figure 10 illustrates the monthly precipitation (in mm) over ten years from 2026 to 2035. Precipitation is highly seasonal, with the majority of rainfall occurring in the first few months of the year (January to April) and towards the end of the year (November and December), while the middle months (May to October) experience significantly lower rainfall. The highest precipitation levels are observed in January, where some years record values exceeding 70 mm, while February and March also display relatively high rainfall but with greater variability across different years. The months from June to September exhibit almost negligible precipitation, indicating a dry period. A noticeable variation in precipitation patterns is observed across the different years, particularly in peak rainfall months. For example, some years, such as 2026 and 2035, show pronounced rainfall in December, while others, like 2029 and 2030, experience peaks in March and April. This suggests interannual variability, which could be influenced by climate patterns or local meteorological conditions. Additionally, the month of November demonstrates moderate rainfall levels, showing an increase compared to the preceding dry months. Overall, the data highlights a clear seasonality in precipitation, with distinct wet and dry periods that may have implications for water resource management, agriculture, and climate adaptation strategies.

Monthly temperature variations (°C) are shown in Figure 11 for the ten years from 2026 until 2035. It seems that during the early months of the year (January and February) and the end of the year (November and December), lower temperatures are observed; on the other hand, peak temperatures occur in the middle months (May to September). This pattern reinforces a standard climatic cycle in which temperatures increase gradually from winter to summer, peaking in June, July, and August before coming down toward the frigid end of the year.

Different years show similarly, which is expected when looking at temperature values. The summer months, especially June, July, and August, consistently record temperatures above 40°C, showing a hot summer. In contrast, the cold months, primarily January and December, transpire at lower temperatures, typically between 15°C and 25°C, while the transitional months of March, April, October, and November witness moderate temperatures, connecting the seasonal extremes.

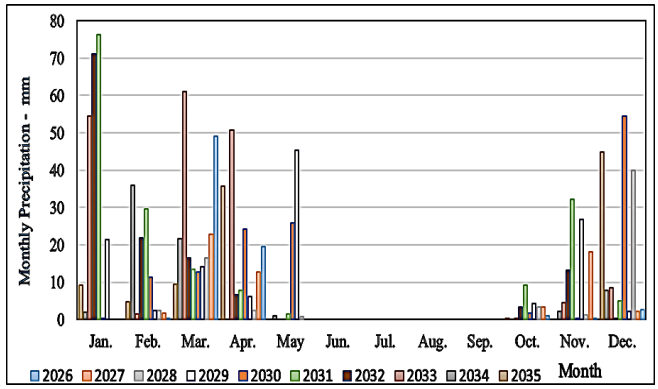


**Figure 10.** Monthly precipitation (mm) within the study area for the period (2026–2035)

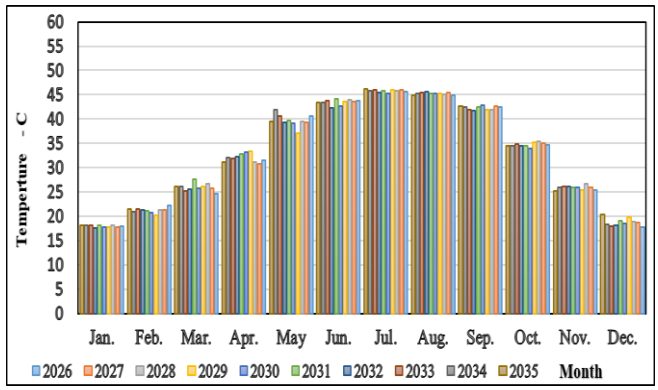


**Figure 11.** Average maximum monthly temperature (°C) for the period (2026–2035)

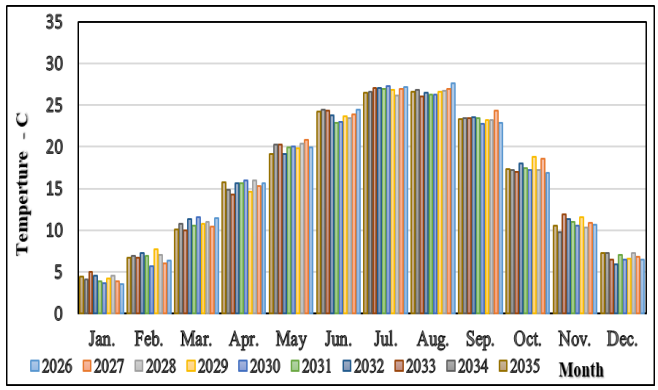


**Figure 12.** Average minimum monthly temperature (°C) for the period (2026–2035)

In summary, this figure demonstrates that there is a clear annual temperature cycle with seasonal trends that are almost predictable. Your research is based on data collected until October 2023. Furthermore, the small changes from year to year reveal an overall steady climate with few major temperature anomalies over the time frame analyzed.

10-year periods of monthly temperatures (°C) for 2026-2035 are shown in Figure 12. Both discovered a distinct seasonal pattern, with a lower mean temperature found in winter months (January, February, November, December) and a higher mean temperature in summer months (June, July, and

August). From January, the temperature slowly rises, reaching its peak in the months of June and July and falling back again by the end of the year, exhibiting a very distinct climatic cycle.

The summer months are relatively constant, with June, July, and August recording the highest temperatures consistently above 25°C to almost 30°C. Lows are seen in December, January, and February, with registered or recorded temperatures usually not exceeding values less than 10°C in some cases, indicating winter months. The transient months like March, April, September, and October show average temperature levels and act as a transition between extreme summer and winter.

In particular, there is little variation in temperature between the different years, which indicates stable long-term climatic conditions in the region. This suggests that during the period studied, there were no extreme temperature anomalies or temporal trends/changes seen. Other areas affected by the temperature cycle shown in the graphic include agriculture, energy use, and climate adaptation planning, as clearly defined warm and cold months shape heating and cooling needs, water availability, and crop growth patterns.

### 6.2 SWAT model results

The hydrological model (SWAT) was operating for estimation and predicting the future surface runoff for Hiqlan Valley. The ability of this model in predicting surface runoff for the next years (future period) depended upon the availability of input data such as the future weather data (rain, temperature, and radiation), DEM, the land cover maps, and all other data required in model operation. The results of the SWAT model operating represent the simulated and predicted Surface Runoff in the next 10 years, period (2026–2035) for Hiqlan Valley, as shown in Figures 13 and 14 for annual surface runoff as depth in (mm) and as volume in ($Mm^3$). In addition, Figure 15 shows results for the expected future monthly surface runoff as depth. The Annual Surface Runoff (A.S.R.O.) depth from 2026 to 2035 is shown in Figure 13. There are significant variations in recorded depth throughout the data, with the highest depth logged in 2028, followed by a decrease in 2029 and more fluctuations in the years after. The peak in 2028 indicates a year of higher surface runoff—likely resulting from elevated precipitation, extreme weather events, or land-use changes impacting watershed hydrology. Variations over the years suggest that the depth of the composition is not regular and it is probably influenced by the climate regime, the seasonal distribution of rainfall, as well as by the specific characteristics of the watershed, like the soil infiltration capacity or vegetation cover.

A part of the graph of annual surface runoff volume is shown in Figure 14 for the same period. The trend lags the depth variations closely, with peak runoff volume again being in 2028, with a sharp increase in runoff almost matching the peak in the depth chart. This is indicative that depth and total runoff volume are closely related and are likely responding to similar climatic and hydrological drivers. The year-to-year variability in A.S.R.O. volume also illustrates the highly variable nature of surface runoff, which may respond to changes in rainfall intensity, land use, and water management. The rises and drops or runs in the data indicate that while climate change is a major factor, there are still seasonal changes in rainfall events and runoff response, which means there will still be other contributing variables in water planning strategies and infrastructure design, especially with the potential for extreme event run-off.

Figure 15 shows that the expected future monthly runoff does not occur in several months for each year, except for a few months in the winter season (rainy season) from November to January, and in the spring season from March to April, with different values of runoff quantity. These results are very important for knowing the quantities of water for the future periods that are expected to come from the Hiqlan Valley, which feeds the Euphrates River. The data related to the expected quantity of surface runoff as additional water in the next years from this valley is considered important information in the water resources management plans for the Euphrates River basin, since this river suffers from a shortage and lack of water supplies that come from the Syrian border.

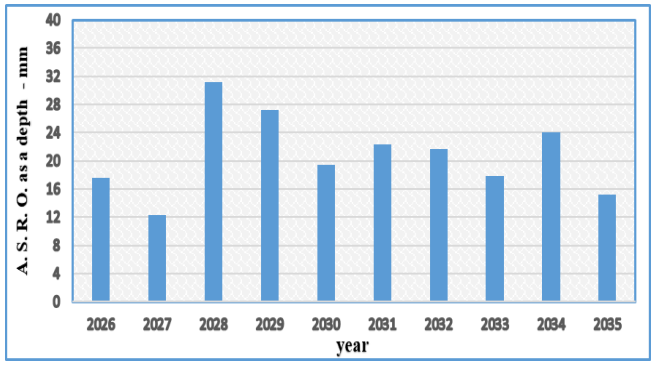


**Figure 13.** Annual surface runoff as depth (mm) for Hiqlan Valley in the period (2026–2035)

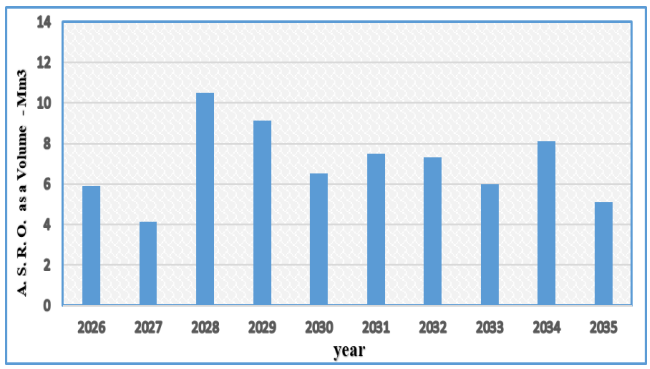


**Figure 14.** Annual surface runoff as volume ($mm^3$) for Hiqlan Valley in the period (2026–2035)

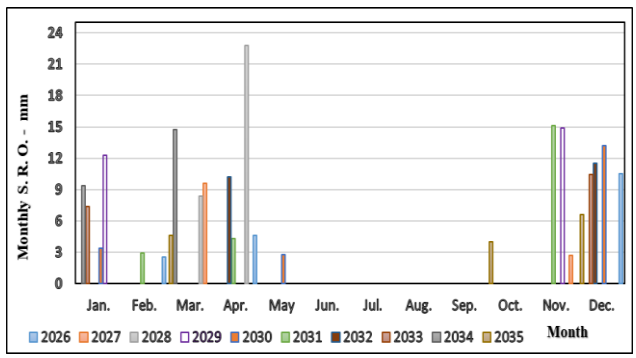


**Figure 15.** Expected future monthly surface runoff as depth in (mm) prediction by the SWAT model (2026–2035)

## 7. CONCLUSIONS

From the analysis of the results, the following key conclusions can be drawn from this study:

- The generated future weather data indicates that maximum precipitation occurs in January (2031) at 76.4 mm, March (2033) at 61.1 mm, April (2033) at 50.7 mm, and December (2030) at 54.5 mm, while the summer months exhibit minimal or no precipitation. This seasonal concentration of rainfall underscores the need for effective water storage and flood management strategies.
- The expected maximum surface runoff occurs in January (2029) at 12.3 mm, November (2031) at 15.1 mm, and December (2030) at 13.2 mm in the winter season, March (2034) at 14.7 mm, and April (2028) at 22.8 mm in the spring season, as per simulations by the SWAT model.
- Based on the next decade's projected monthly surface runoff from Hiqlan Valley, it can be concluded that runoff events will occur two to four times per year. This frequency of runoff events indicates the intermittent nature of water availability in the region, which is crucial for hydrological planning and agricultural water management.
- The results show distinct seasonality in precipitation and temperature over the decade. In contrast, temperature follows a steady annual cycle, with higher temperatures in the summer and lower temperatures in winter, whereas precipitation is very variable and concentrated in the first and last months of the year. These reliable seasonal patterns allow for useful predictions of water resource management, energy needs, and agricultural planning.
- The study's intermixed outcomes reveal a direct influence of future climate conditions on hydrological behavior, signaling the need for proactive approaches towards ensuring sustainable planning of water resources. Future mitigation, agriculture, and water conservation efforts in the region will benefit from the integrated approaches that account for climate variability, precipitation distribution, and runoff characteristics.
- There is a necessity to construct runoff and surface flow field measuring and monitoring stations for the valleys situated on the right side of the Euphrates River in the western desert area.


## ACKNOWLEDGEMENTS

The authors express their sincere gratitude to the University of Baghdad, College of Engineering, Department of Water Resources Engineering, for their invaluable support.


## REFERENCES


[1] Farhan, A.A., Abed, B.S. (2022). Numerical modelling of surface runoff in watershed areas related to Bahr AL-Najaf. In Geotechnical Engineering and Sustainable Construction: Sustainable Geotechnical Engineering, pp. 241-251. https://doi.org/10.1007/978-981-16-6277-5_20

[2] Al-Juhaishi, M.R., Oleiwi, A.S., Aed, B.S. (2024). Modeling surface runoff in Al-Mohammadi Valley: Influence of climate and soil parameters. International Journal of Design and Nature and Ecodynamics, 19(3): 1043-1049. https://doi.org/10.18280/ijdne.190333

[3] Hussein, A.K., Muneam, R.R., Jafer, N.A., Ibrahimand, A.A., Abojassim, A.A. (2023). Surface water assessment using water quality index: A case study of the Euphrates River, Najafi, Iraq, by using the GIS Technique. IOP Conference Series: Earth and Environmental Science, 1225(1): 012012. https://doi.org/10.1088/1755-1315/1225/1/012012

[4] Oleiwi, A.S., Abed, B.S., Hasan, B.F. (2023). Rainfall prediction and runoff modelling under climate change scenarios for Tigris River from Mosul to Baghdad cities. International Journal of Design & Nature and Ecodynamics, 18(3): 537-546. https://doi.org/10.18280/ijdne.180305

[5] Yousuf, A., Manzoor, S.O. (2020). Permeability of multi-layered soils for flow perpendicular to bedding plane. i-manager's Journal on Future Engineering and Technology, 15(4): 1-7. https://doi.org/10.26634/jfet.15.4.17118

[6] Saleh, R.A.Q., Oleiwi, A.S., Lateef, Z.Q. (2024). The impact of climate change on water quality and consumption in the Tigris River Basin (Mosul-Baghdad). IOP Conference Series: Earth and Environmental Science, 1374(1): 012048. https://doi.org/10.1088/1755-1315/1374/1/012048

[7] Al-Marj, O.K., Naeem, S.M., Lateef, H.A. (2025). Predicted model of water storage: A case study in Basra City, Iraq. Mathematical Modelling of Engineering Problems, 12(1): 227-240. https://doi.org/10.18280/mmep.120124

[8] Mohammed, Z.M., Hassan, W.H. (2022). Climate change and the projection of future temperature and precipitation in southern Iraq using a LARS-WG model. Modeling Earth Systems and Environment, 8(3): 4205-4218. https://doi.org/10.1007/s40808-022-01358-x

[9] Hassan, W.H., Nile, B.K., Kadhim, Z.K., Mahdi, K., Riksen, M., Thiab, R.F. (2023). Trends, forecasting and adaptation strategies of climate change in the middle and west regions of Iraq. SN Applied Sciences, 5(12): 312. https://doi.org10.1007/s42452-023-05544-z

[10] Al-Kubaisi, M.H., Al-Kubaisi, Q.Y. (2023). Using SWAT model to estimate the water balance of Wadi Al-Mohammadi Basin, Western Iraq. Iraqi Journal of Science, 64(3): 1254-1267. https://doi.org/10.24996/ijs.2023.64.3.21

[11] Zubaidi, S.L., Kot, P., Hashim, K., Alkhaddar, R., Abdellatif, M., Muhsin, Y.R. (2019). Using LARS–WG model for prediction of temperature in Columbia City, USA. IOP Conference Series: Materials Science and Engineering, 584(1): 012026. https://doi.org/10.1088/1757-899X/584/1/012026

[12] Karimi, S., Karimi, S., Yavari, A.R., Niksokhan, M.H. (2015). Prediction of temperature and precipitation in Damavand catchment in Iran by using LARS–WG in future. Earth Sciences, 4(3): 95-100. https://doi.org/10.11648/j.earth.20150403.12

[13] Arnold, J.G., Kiniry, J.R., Srinivasan, R., Williams, J.R., Haney, E.B., Neitsch, S.L. (2011). Soil and water assessment tool input/output file documentation version 2009. Texas Water Resources Institute.

[14] Farhan, A.M., Al Thamiry, H.A. (2020). Estimation of the surface runoff volume of Al-Mohammedi valley for

long-term period using SWAT model. Iraqi Journal of Civil Engineering, 14(1): 8-12. https://doi.org/10.37650/ijce.2020.172870
[15] Farhan, A.A., Abed, B.S. (2021). Estimation of surface runoff to Bahr Al-Najaf. Journal of Engineering, 27(9): 51-63. https://doi.org/10.31026/j.eng. 2021.09.05
[16] Ang, R., Oeurng, C. (2018). Simulating streamflow in an ungauged catchment of Tonle sap Lake Basin in Cambodia using (SWAT). Water Science, 32(1): 89-101. https://doi.org/10.1016/j.wsj.2017.12.002
[17] Gassman, P.W., Reyes, M.R., Green, C.H., Arnold, J.G. (2007). The soil and water assessment tool: Historical development, applications, and future research directions. Transactions of the ASABE, 50(4): 1211-1250. https://doi.org/10.13031/2013.23637
[18] Teshager, A.D., Gassman, P.W., Secchi, S., Schoof, J.T., Misgna, G. (2016). Modeling agricultural watersheds with the soil and water assessment tool (SWAT): Calibration and validation with a novel procedure for spatially. Environmental Management, 57: 894-911. https://doi.org/10.1007/s00267-015-0636-4
[19] Al-Kubaisi, Q.Y., Rasheed, A.A. (2017). Using annual rainfall to estimate the surface runoff and groundwater recharge in Lialan Basin (Southeast Kirkuk-North of Iraq). Iraqi Journal of Science, 58(4B): 2128-2138. https://doi.org/10.24996/ijs.2017.58.4B.17
[20] Ware, H.H., Chang, S.W., Lee, J.E., Chung, I.M. (2024). Assessment of hydrological responses to land use and land cover changes in forest-dominated watershed using SWAT model. Water, 16(4): 528. https://doi.org/10.3390/w16040528
[21] Mahmoodi, M., Honarmand, M., Naseri, F., Mohammadi, S. (2020). The effect of land use changes on the flood hydrograph in the Kashaf-Rood River by analyzing of SCS-CN results. Water and Soil, 34(1): 43-54. https://doi.org/10.22067/jsw.v34i2.84342
[22] Khalaf, A.G., Mohammed, G.H., Jaseem, A.A. (2016). Monitoring change of marshes in South of Iraq by using image processing techniques for Landsat images through period from 1990 to 2015. Journal Engineering Technology, 34: 261-274.
[23] Kadhim, M.M. (2018). Monitoring land cover change using remote sensing techniques: A case study of Dalmaj marsh, Iraq. Journal of Engineering, 24(9): 96-108. https://doi.org/10.31026/j.eng.2018.09.07
[24] Al-Jawad, M.S., Ahmed, I.J. (2018). Permeability estimation by using the modified and conventional FZI methods. Journal of Engineering, 24(3): 59-67. https://doi.org/10.31026/j.eng.2018.03.05
[25] Kalcic, M.M., Chaubey, I., Frankenberger, J. (2015). Defining soil and water assessment tool (SWAT) hydrologic response units (HRUs) by field boundaries. International Journal of Agricultural and Biological Engineering, 8(3): 69-80.
[26] Mustafa, A.S., Sulaiman, S.O., Hussein, O.M. (2016). Application of SWAT model for sediment loads from valleys transmitted to Haditha reservoir. Journal of Engineering, 22(1): 184-197. https://doi.org/10.31026/j.eng.2016.01.12
[27] Talib, Z.R., Laffta, S.J. (2024). Effect of climate change on land cover (case study: Hilla district). Journal of Engineering, 30(8): 136-148. https://doi.org/10.31026/j.eng.2024.08.09
[28] Shukur, H.K. (2017). Estimation curve numbers using GIS model. Journal of Engineering, 23(5): 1-11. https://doi.org/10.31026/j.eng.2017.05.01
[29] Sulaiman, S.O., Mahmood, N.S., Kamel, A.H., Al-Ansari, N. (2021). The evaluation of the SWAT model performance to predict the runoff values in the Iraqi western desert. Environment and Ecology Research, 9(6): 330-339. https://doi.org/10.13189/eer.2021.090602
[30] Samson, T.K., Aweda, F.O. (2024). Seasonal autoregressive integrated moving average modelling and forecasting of monthly rainfall in selected African stations. Mathematical Modelling of Engineering Problems, 11(1): 159-168. https://doi.org/10.18280/mmep.110117
[31] Shaikh, M.M., Lodha, P.P., Eslamian, S. (2022). Automatic calibration of SWAT hydrological model by SUFI-2 algorithm. International Journal of Hydrology Science and Technology, 13(3): 324-334. https://doi.org/10.1504/IJHST.2021.10036580